Electronic Supplementary Material (ESI) for RSC Advances.

Supporting Information

Supramolecular thermogels from branched PCL-containing polyurethanes

Qianyu Lin[b], Jason Y. C. Lim[a], Kun Xue[a], Celestine P. T. Chee[a], Xian Jun Loh*[a]

[a] Prof. (Dr.), X.J., Loh*, Dr. J.Y.C. Lim, Dr. K. Xue, C. P. T. Chee
Soft Materials Department
Institute of Materials Research and Engineering, Agency for Science, Technology and Research (A*STAR)
Address: 2 Fusionopolis Way, Innovis, Singapore 138634
E-mail: lohxj@imre.a-star.edu.sg

[b] Q., Lin
NUS Graduate School for Integrative Sciences and Engineering
National University of Singapore
21 Lower Kent Ridge Rd, Singapore 119077

S1. Degree of Discrimination between PPG and PEG blocks during Polyurethane Synthesis

Table S1. Relative Integration of PPG and HMDI resonances at different durations of reaction

Duration/ min	Relative ^{1}H NMR Integration		Mole ratio	
	PPG[a]	HMDI[b]	PPG	HMDI
10	7.31	1	0.287	1
15	7.49	1	0.294	1
20	7.36	1	0.289	1
25	7.43	1	0.291	1
30	7.36	1	0.289	1
40	7.69	1	0.302	1
50	7.49	1	0.294	1
60	7.43	1	0.291	1
90	7.33	1	0.287	1
105	7.39	1	0.290	1
120	7.51	1	0.295	1
180	7.56	1	0.296	1
210	7.56	1	0.296	1
240	7.71	1	0.302	1
300	7.76	1	0.304	1
360	7.62	1	0.299	1

[a] Resonance at 1.10-1.15 ppm [b] Resonance at 3.10-3.15 ppm

S2. CMC determination for Thermogelling Polyurethanes

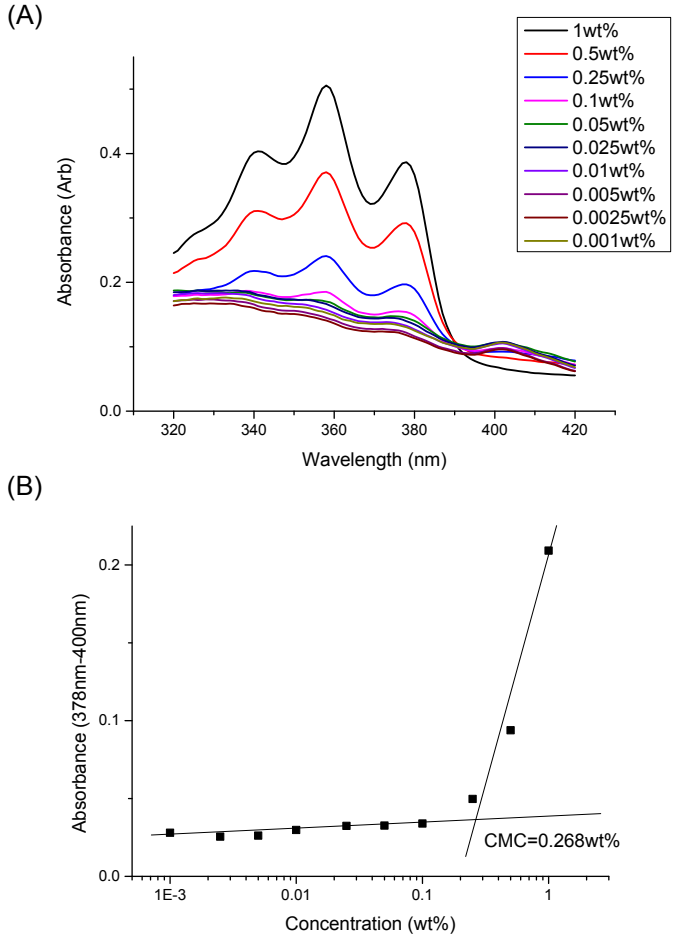

Figure S1. (A) UV-Vis absorbance spectra of DPH dye at different concentrations of polymer 1P30-1h at 15°C; (B) Difference in DPH absorbance at 378 and 400 nm as a function of concentration of 1P30-1h at 15°C. The CMC was determined by the intersection of the extrapolated linear best fit lines at low and high concentrations of polymer.

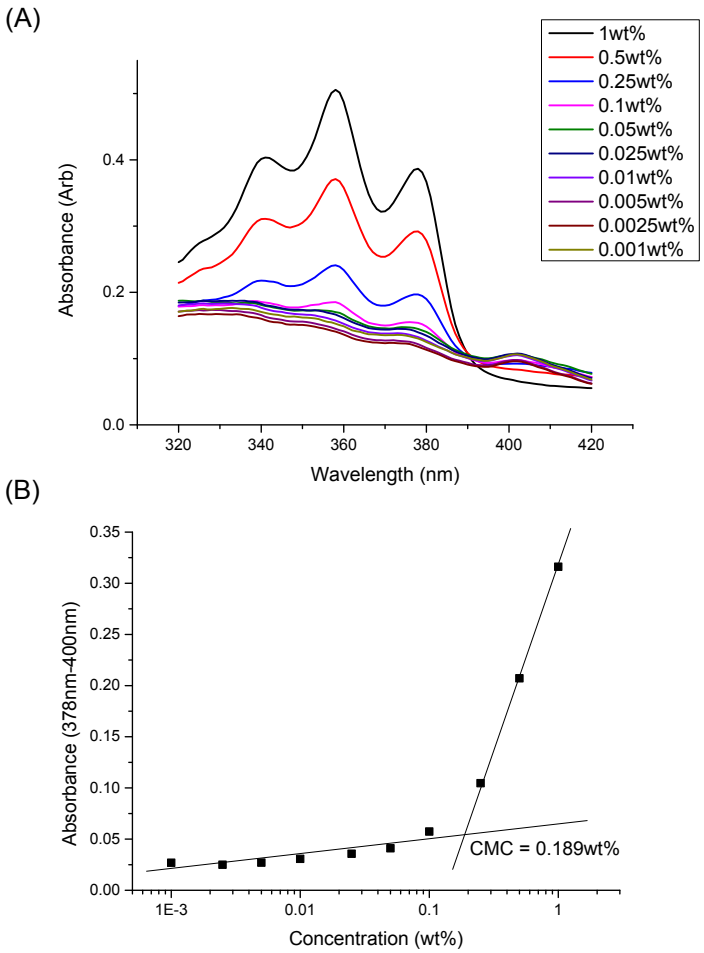

Figure S2. (A) UV-Vis absorbance spectra of DPH dye at different concentrations of polymer 1P30-1h at 25°C; (B) Difference in DPH absorbance at 378 and 400 nm as a function of concentration of 1P30-1h at 25°C. The CMC was determined by the intersection of the extrapolated linear best fit lines at low and high concentrations of polymer.

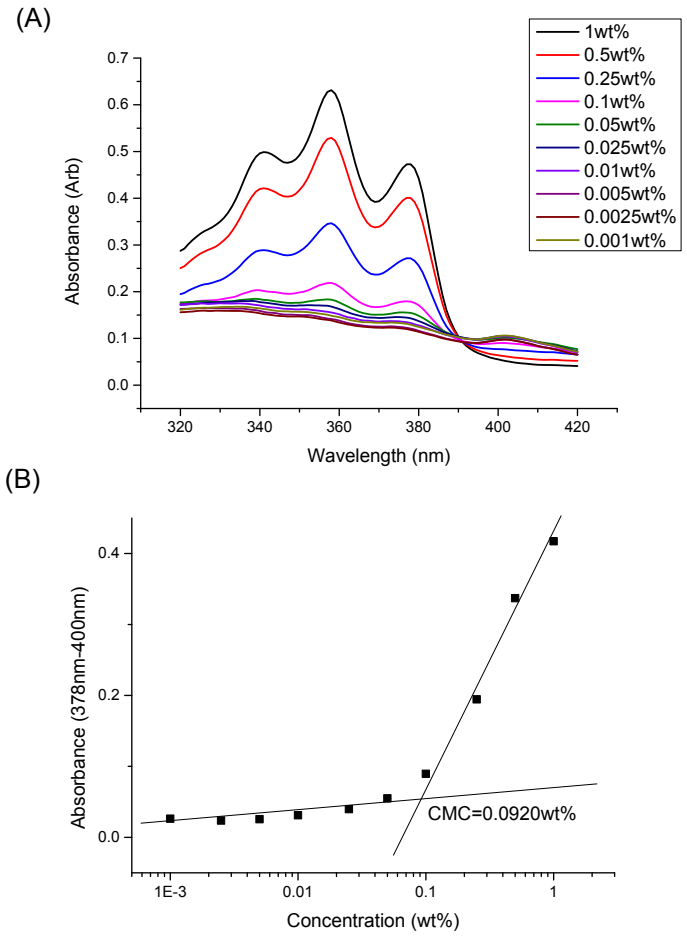

Figure S3. (A) UV-Vis absorbance spectra of DPH dye at different concentrations of polymer 1P30-1h at 35°C; (B) Difference in DPH absorbance at 378 and 400 nm as a function of concentration of 1P30-1h at 35°C. The CMC was determined by the intersection of the extrapolated linear best fit lines at low and high concentrations of polymer.

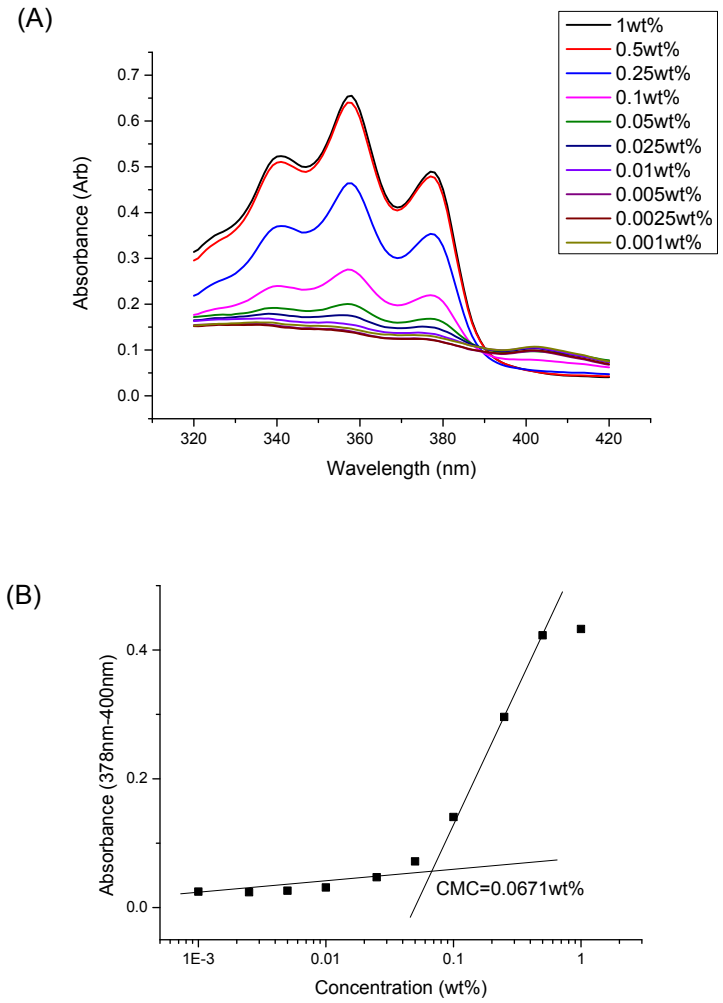

Figure S4. (A) UV-Vis absorbance spectra of DPH dye at different concentrations of polymer 1P30-1h at 45°C; (B) Difference in DPH absorbance at 378 and 400 nm as a function of concentration of 1P30-1h at 45°C. The CMC was determined by the intersection of the extrapolated linear best fit lines at low and high concentrations of polymer.

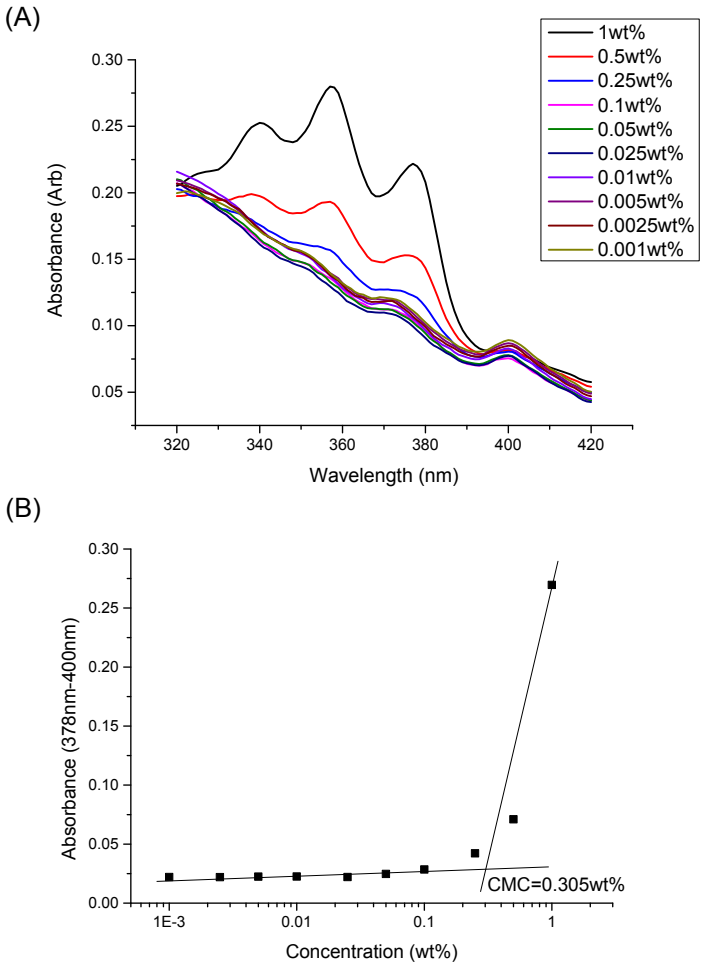

Figure S5. (A) UV-Vis absorbance spectra of DPH dye at different concentrations of polymer 1P30-2h at 15^{o}C; (B) Difference in DPH absorbance at 378 and 400 nm as a function of concentration of 1P30-2h at 15^{o}C. The CMC was determined by the intersection of the extrapolated linear best fit lines at low and high concentrations of polymer.

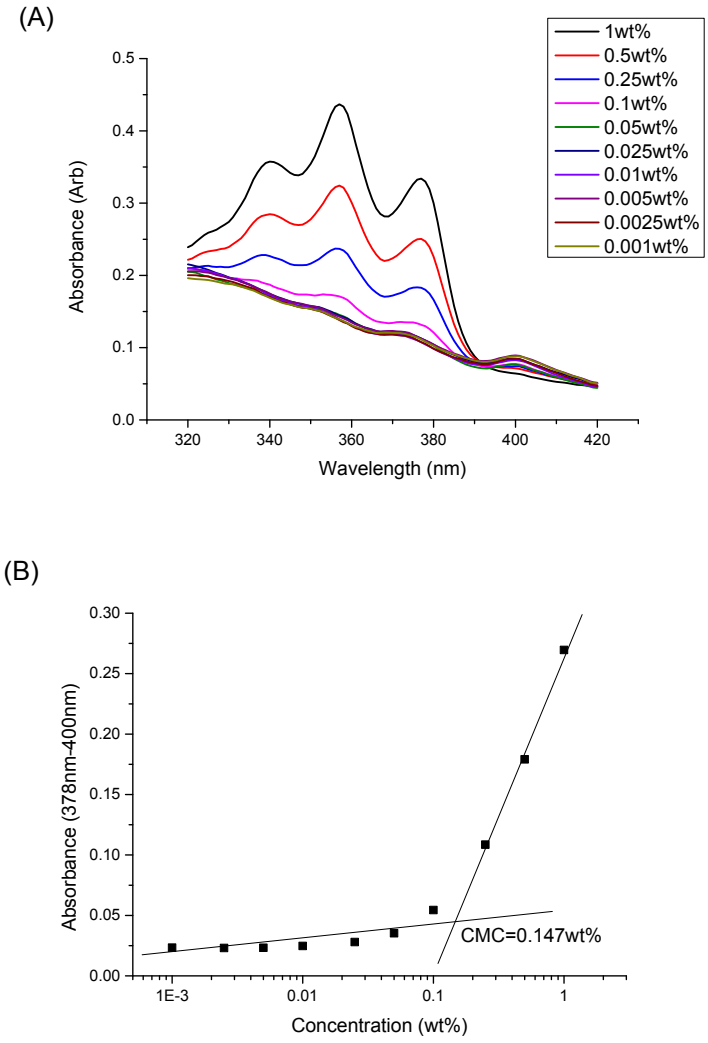

Figure S6. (A) UV-Vis absorbance spectra of DPH dye at different concentrations of polymer 1P30-2h at 25°C; (B) Difference in DPH absorbance at 378 and 400 nm as a function of concentration of 1P30-2h at 25°C. The CMC was determined by the intersection of the extrapolated linear best fit lines at low and high concentrations of polymer.

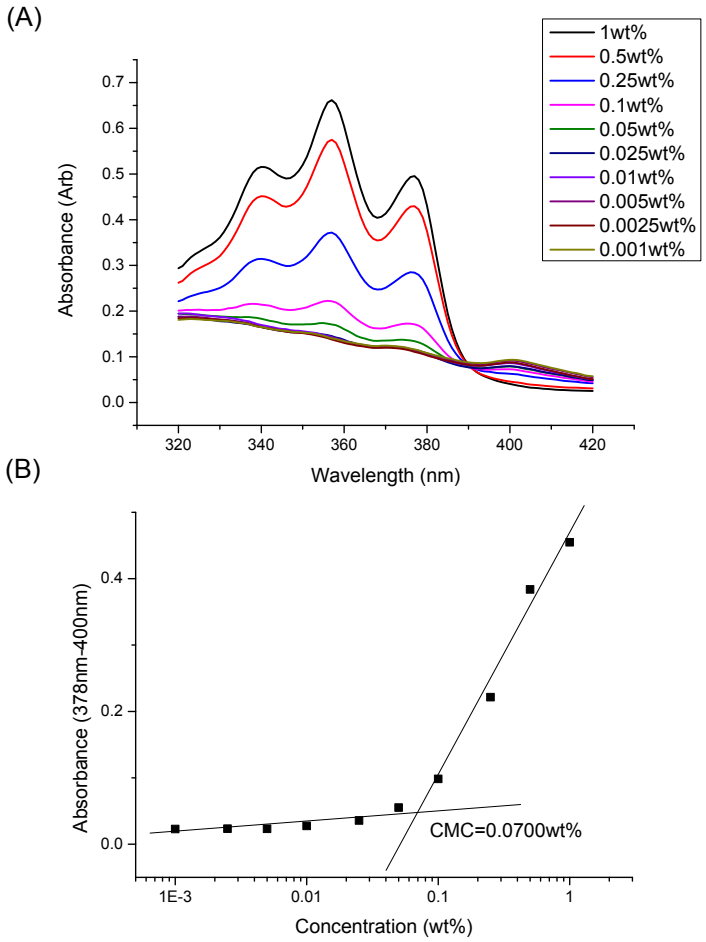

Figure S7. (A) UV-Vis absorbance spectra of DPH dye at different concentrations of polymer 1P30-2h at 35°C; (B) Difference in DPH absorbance at 378 and 400 nm as a function of concentration of 1P30-2h at 35°C. The CMC was determined by the intersection of the extrapolated linear best fit lines at low and high concentrations of polymer.

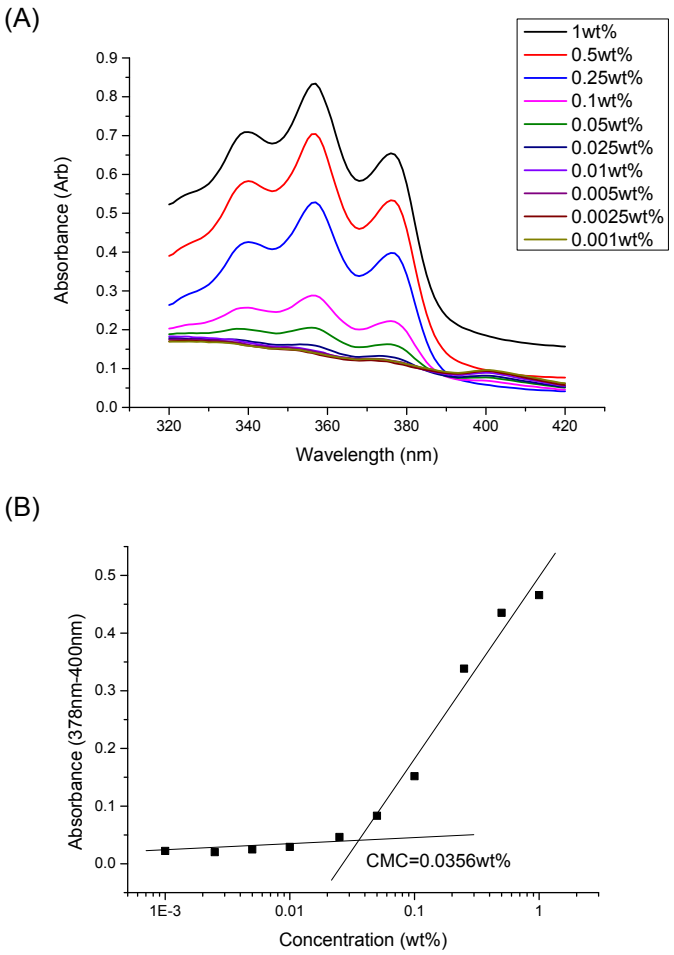

Figure S8. (A) UV-Vis absorbance spectra of DPH dye at different concentrations of polymer 1P30-2h at 45°C; (B) Difference in DPH absorbance at 378 and 400 nm as a function of concentration of 1P30-2h at 45°C. The CMC was determined by the intersection of the extrapolated linear best fit lines at low and high concentrations of polymer.

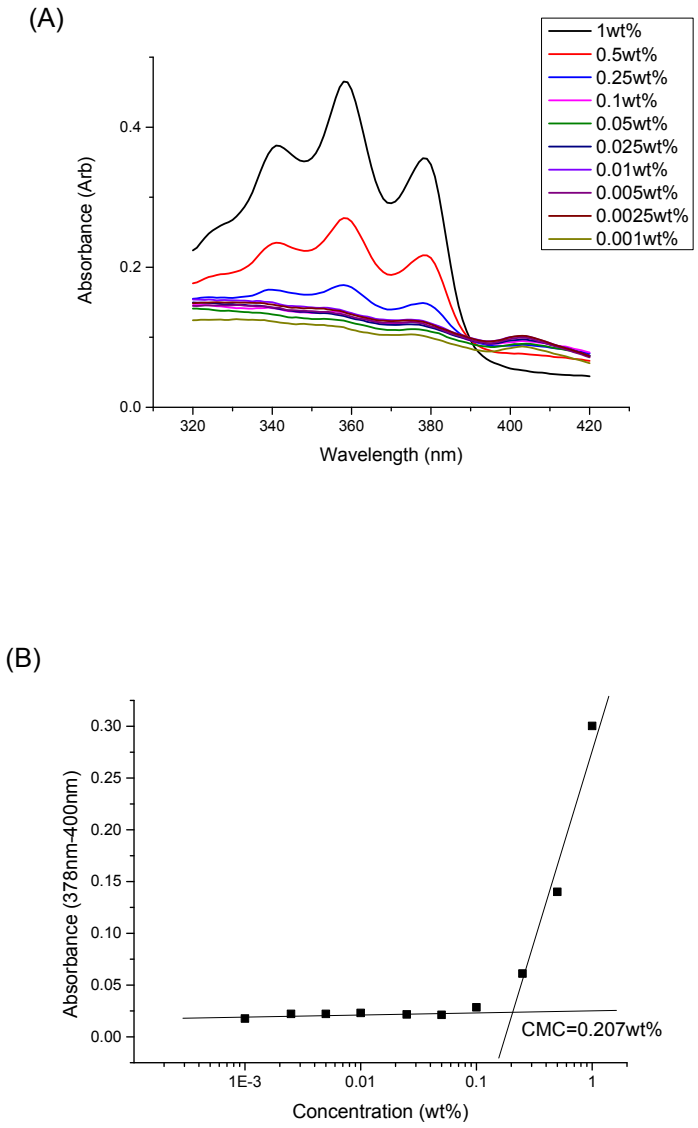

Figure S9. (A) UV-Vis absorbance spectra of DPH dye at different concentrations of polymer 1P30-3h at 15°C; (B) Difference in DPH absorbance at 378 and 400 nm as a function of concentration of 1P30-3h at 15°C. The CMC was determined by the intersection of the extrapolated linear best fit lines at low and high concentrations of polymer.

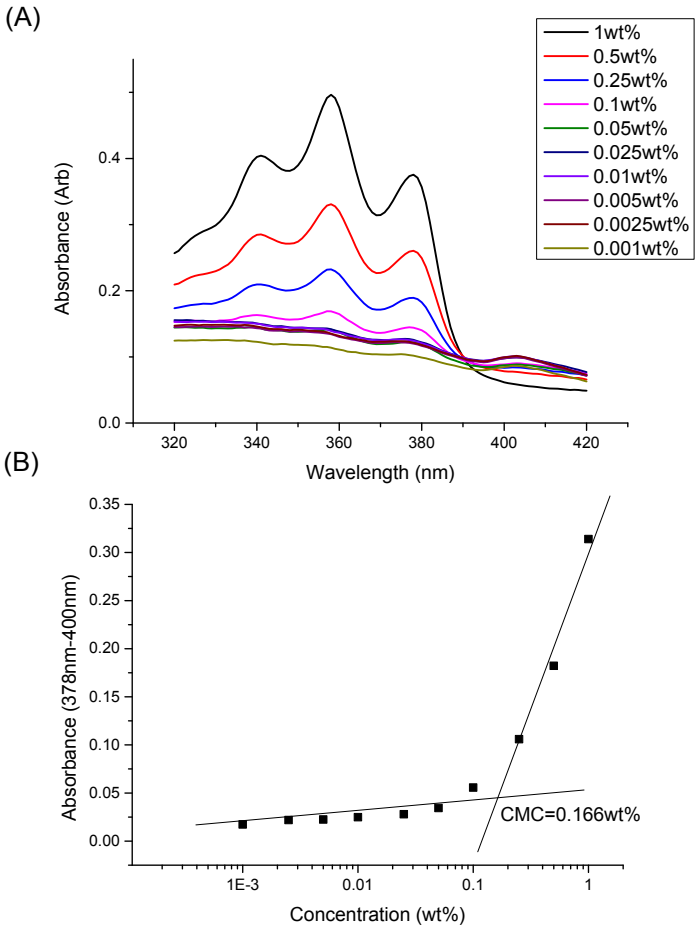

Figure S10. (A) UV-Vis absorbance spectra of DPH dye at different concentrations of polymer 1P30-3h at 25°C; (B) Difference in DPH absorbance at 378 and 400 nm as a function of concentration of 1P30-3h at 25°C. The CMC was determined by the intersection of the extrapolated linear best fit lines at low and high concentrations of polymer.

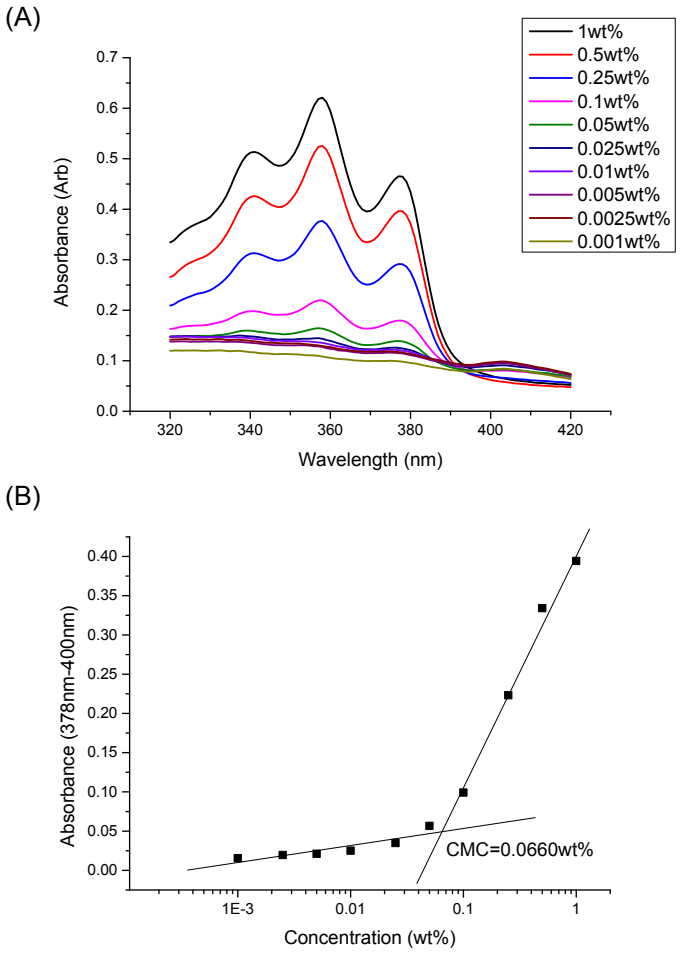

Figure S11. (A) UV-Vis absorbance spectra of DPH dye at different concentrations of polymer 1P30-3h at 35°C; (B) Difference in DPH absorbance at 378 and 400 nm as a function of concentration of 1P30-3h at 35°C. The CMC was determined by the intersection of the extrapolated linear best fit lines at low and high concentrations of polymer.

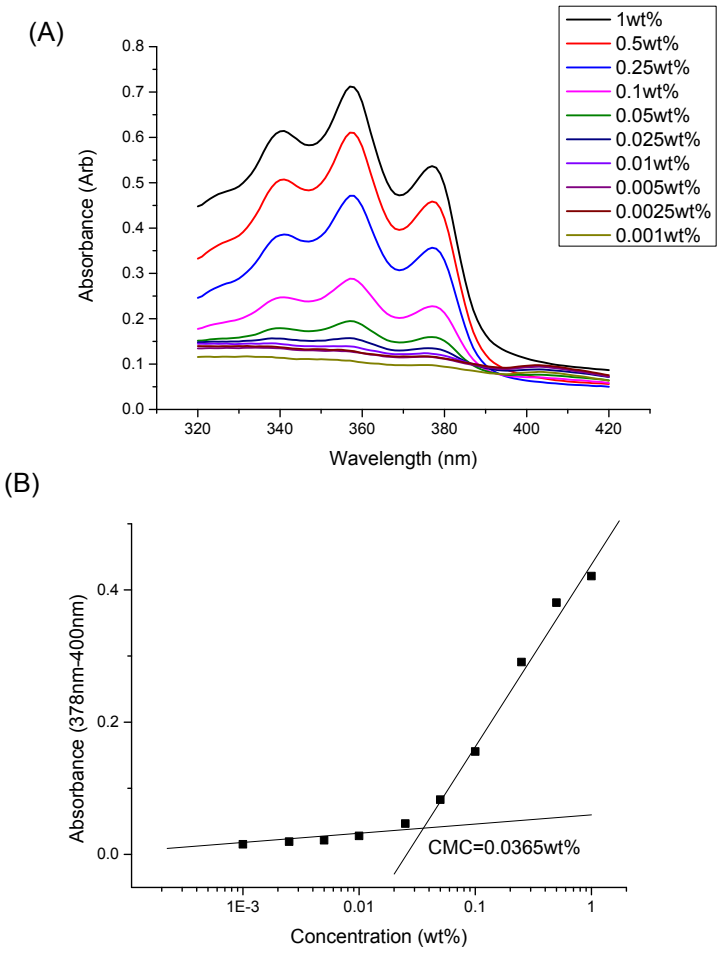

Figure S12. (A) UV-Vis absorbance spectra of DPH dye at different concentrations of polymer 1P30-3h at 45^{o}C; (B) Difference in DPH absorbance at 378 and 400 nm as a function of concentration of 1P30-3h at 45^{o}C. The CMC was determined by the intersection of the extrapolated linear best fit lines at low and high concentrations of polymer.

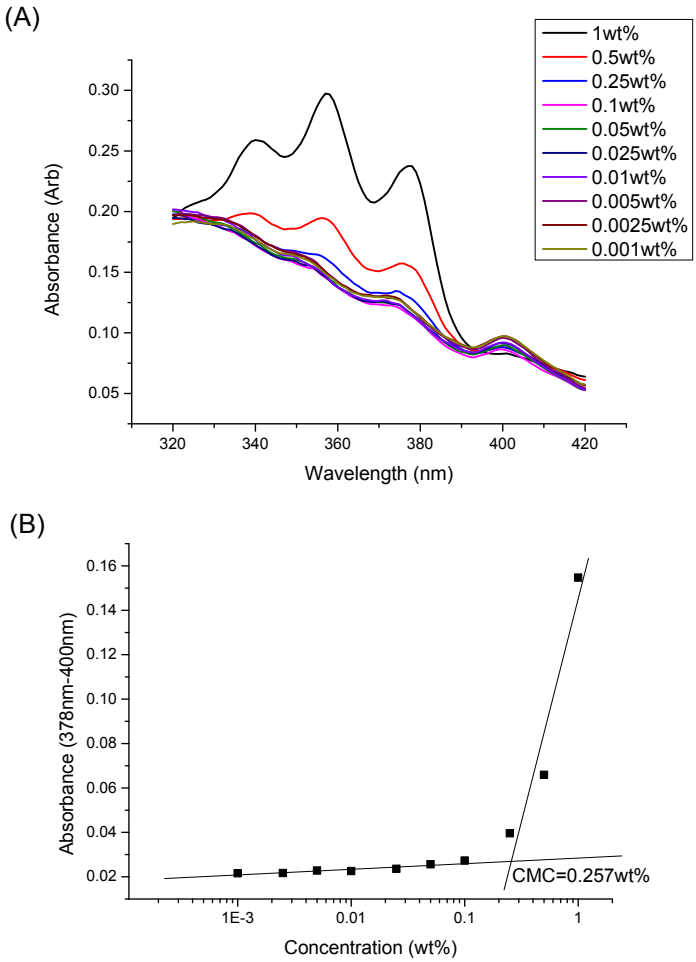

Figure S13. (A) UV-Vis absorbance spectra of DPH dye at different concentrations of polymer 1P35-2h at 15°C; (B) Difference in DPH absorbance at 378 and 400 nm as a function of concentration of 1P35-2h at 15°C. The CMC was determined by the intersection of the extrapolated linear best fit lines at low and high concentrations of polymer.

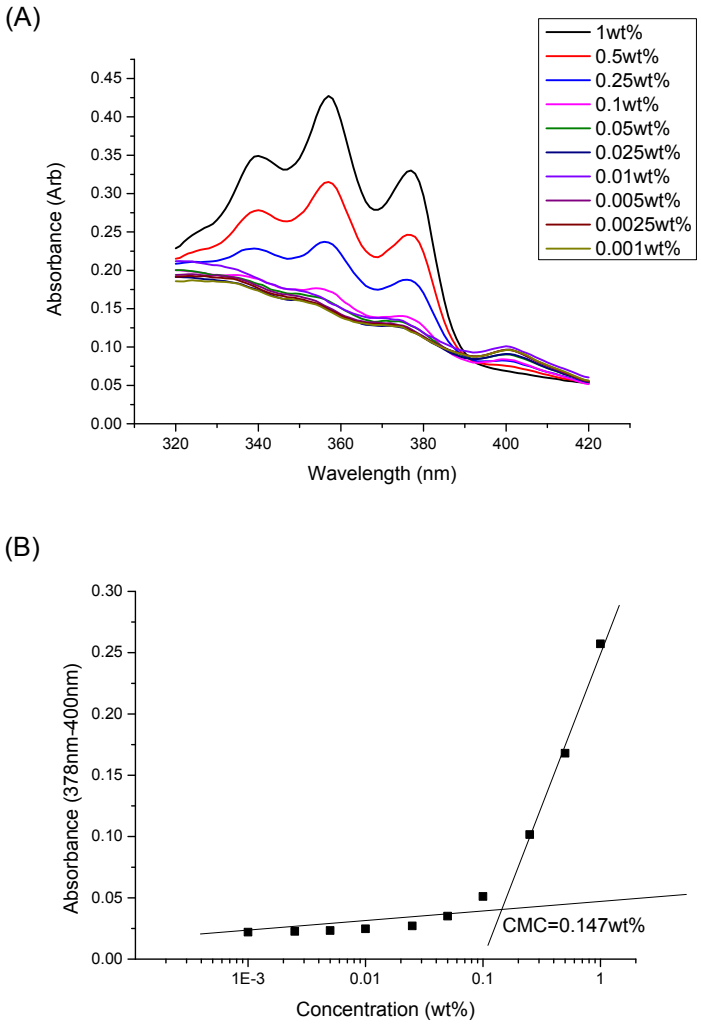

Figure S14. (A) UV-Vis absorbance spectra of DPH dye at different concentrations of polymer 1P35-2h at 25°C; (B) Difference in DPH absorbance at 378 and 400 nm as a function of concentration of 1P35-2h at 25°C. The CMC was determined by the intersection of the extrapolated linear best fit lines at low and high concentrations of polymer.

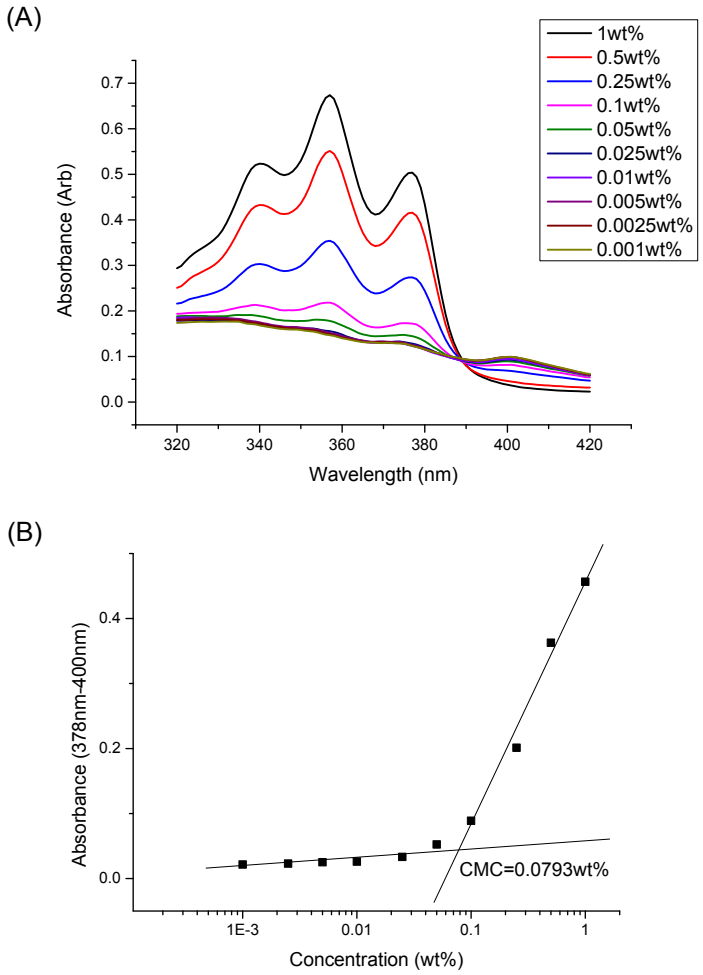

Figure S15. (A) UV-Vis absorbance spectra of DPH dye at different concentrations of polymer 1P35-2h at 35°C; (B) Difference in DPH absorbance at 378 and 400 nm as a function of concentration of 1P35-2h at 35°C. The CMC was determined by the intersection of the extrapolated linear best fit lines at low and high concentrations of polymer.

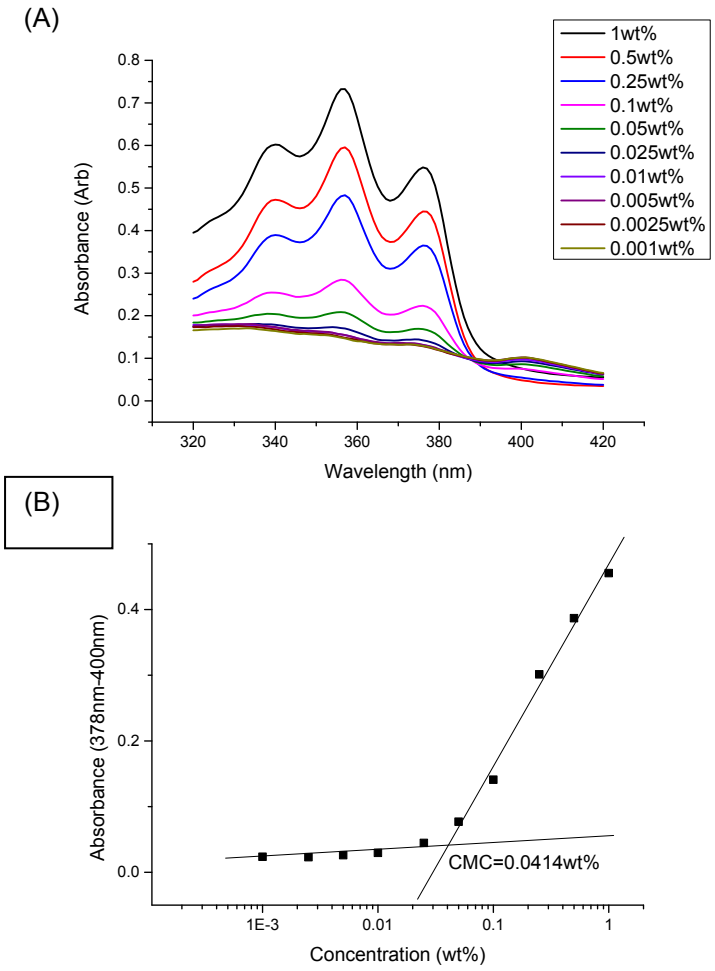

Figure S16. (A) UV-Vis absorbance spectra of DPH dye at different concentrations of polymer 1P35-2h at 45°C; (B) Difference in DPH absorbance at 378 and 400 nm as a function of concentration of 1P35-2h at 45°C. The CMC was determined by the intersection of the extrapolated linear best fit lines at low and high concentrations of polymer.

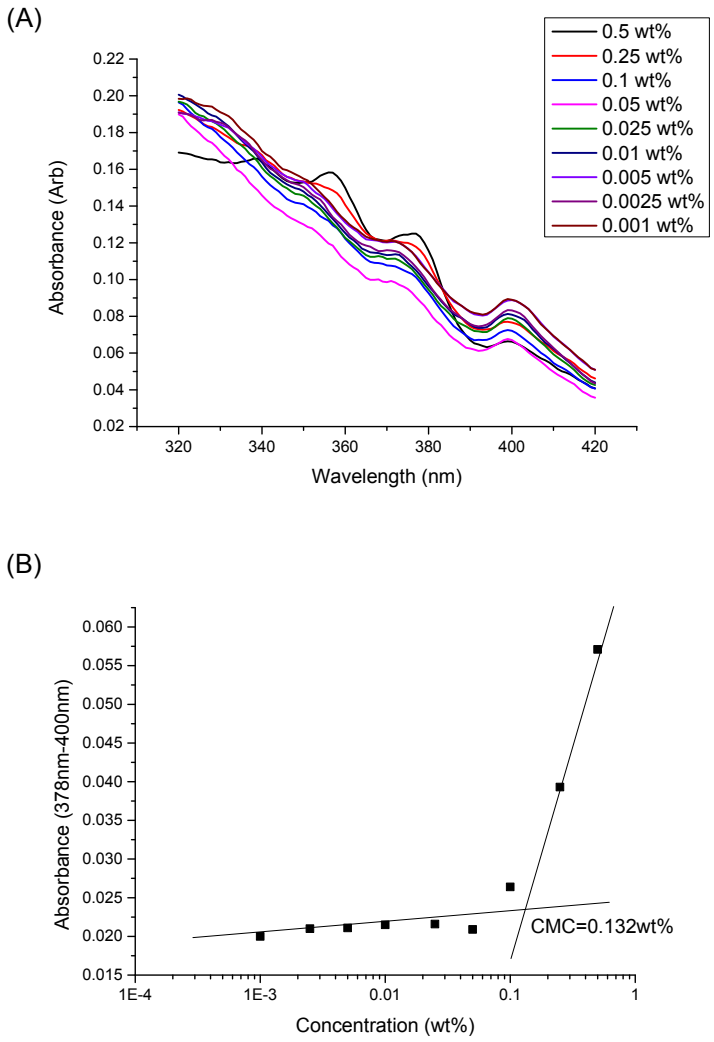

Figure S17. (A) UV-Vis absorbance spectra of DPH dye at different concentrations of polymer 1P35-3h at 15°C; (B) Difference in DPH absorbance at 378 and 400 nm as a function of concentration of 1P35-3h at 15°C. The CMC was determined by the intersection of the extrapolated linear best fit lines at low and high concentrations of polymer.

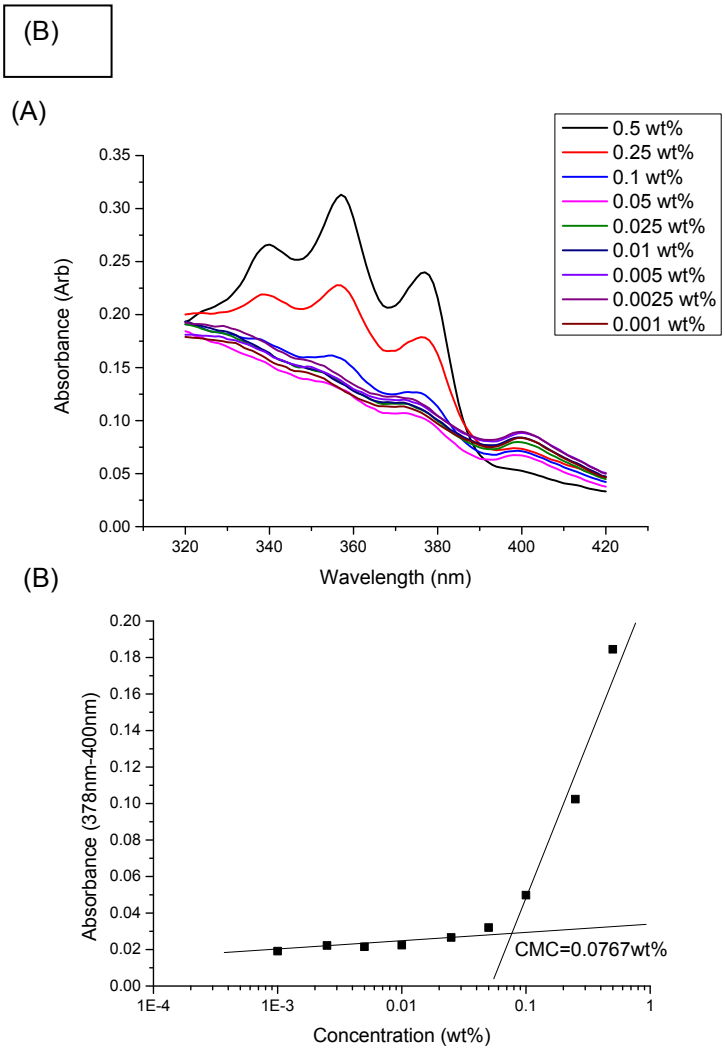

Figure S18. (A) UV-Vis absorbance spectra of DPH dye at different concentrations of polymer 1P35-3h at 25°C; (B) Difference in DPH absorbance at 378 and 400 nm as a function of concentration of 1P35-3h at 25°C. The CMC was determined by the intersection of the extrapolated linear best fit lines at low and high concentrations of polymer.

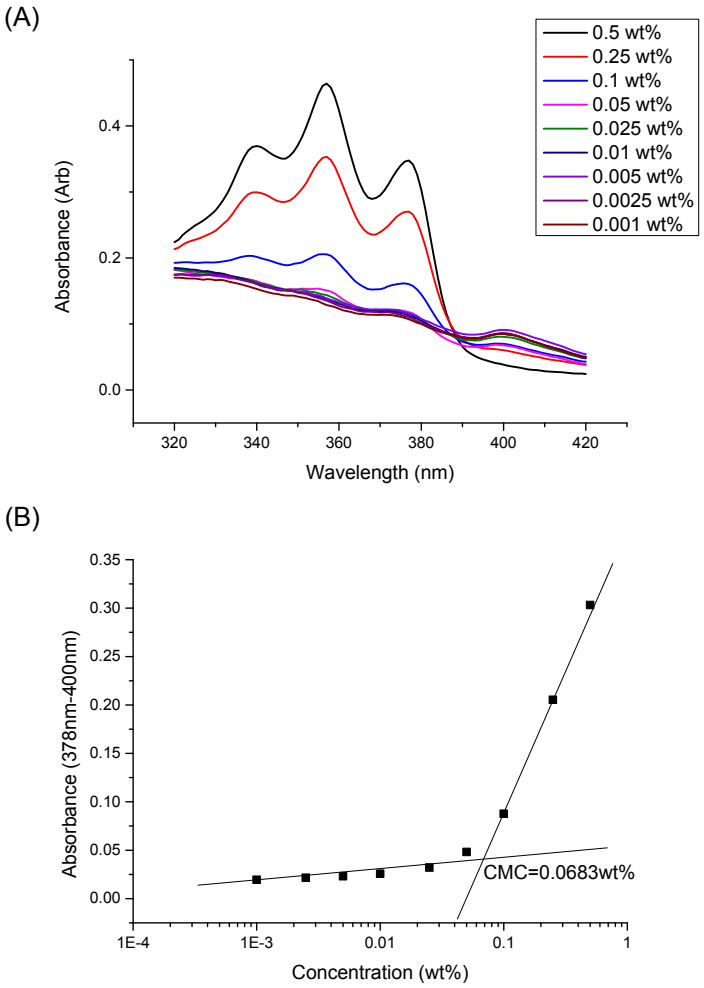

Figure S19. (A) UV-Vis absorbance spectra of DPH dye at different concentrations of polymer 1P35-3h at 35°C; (B) Difference in DPH absorbance at 378 and 400 nm as a function of concentration of 1P35-3h at 35°C. The CMC was determined by the intersection of the extrapolated linear best fit lines at low and high concentrations of polymer.

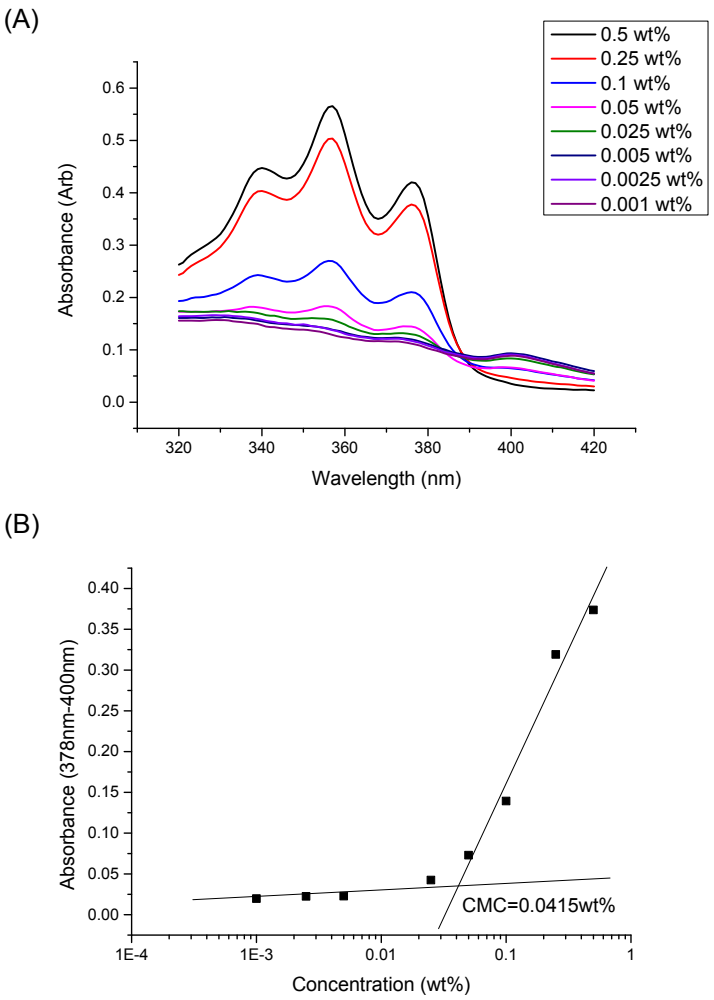

Figure S20. (A) UV-Vis absorbance spectra of DPH dye at different concentrations of polymer 1P35-3h at 45°C; (B) Difference in DPH absorbance at 378 and 400 nm as a function of concentration of 1P35-3h at 45°C. The CMC was determined by the intersection of the extrapolated linear best fit lines at low and high concentrations of polymer.

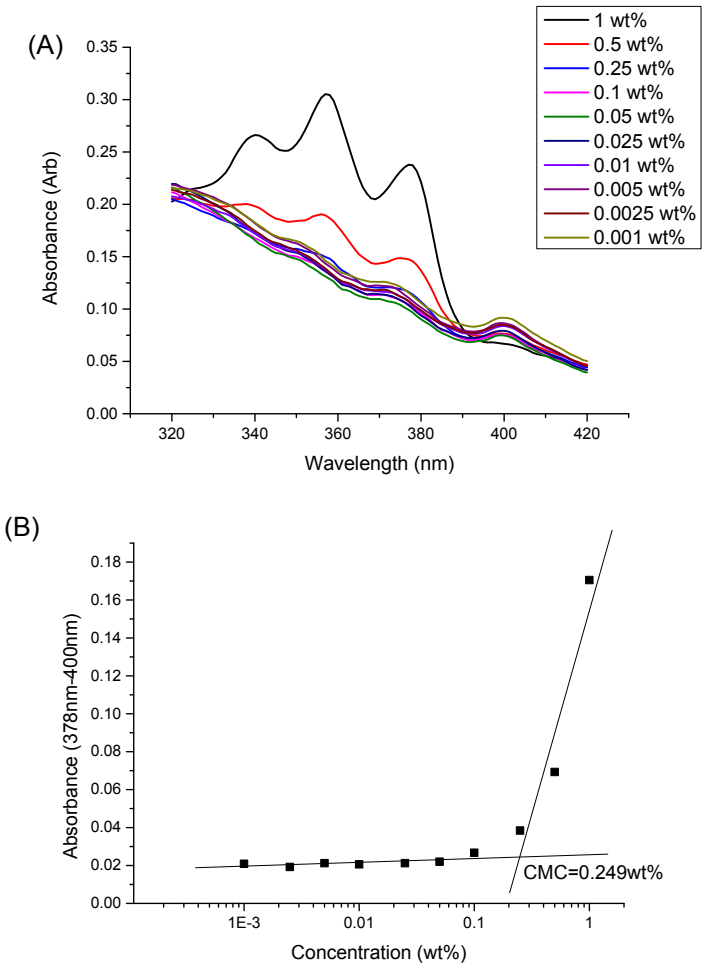

Figure S21. (A) UV-Vis absorbance spectra of DPH dye at different concentrations of polymer 1P35-4h at 15°C; (B) Difference in DPH absorbance at 378 and 400 nm as a function of concentration of 1P35-4h at 15°C. The CMC was determined by the intersection of the extrapolated linear best fit lines at low and high concentrations of polymer.

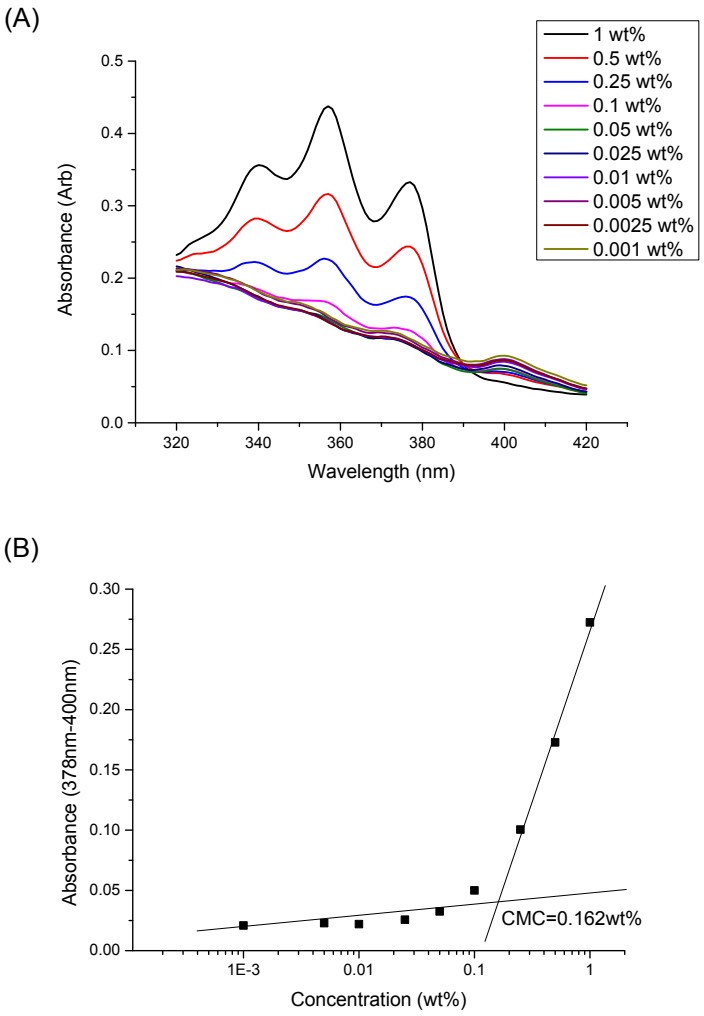

Figure S22. (A) UV-Vis absorbance spectra of DPH dye at different concentrations of polymer 1P35-4h at 25°C; (B) Difference in DPH absorbance at 378 and 400 nm as a function of concentration of 1P35-4h at 25°C. The CMC was determined by the intersection of the extrapolated linear best fit lines at low and high concentrations of polymer.

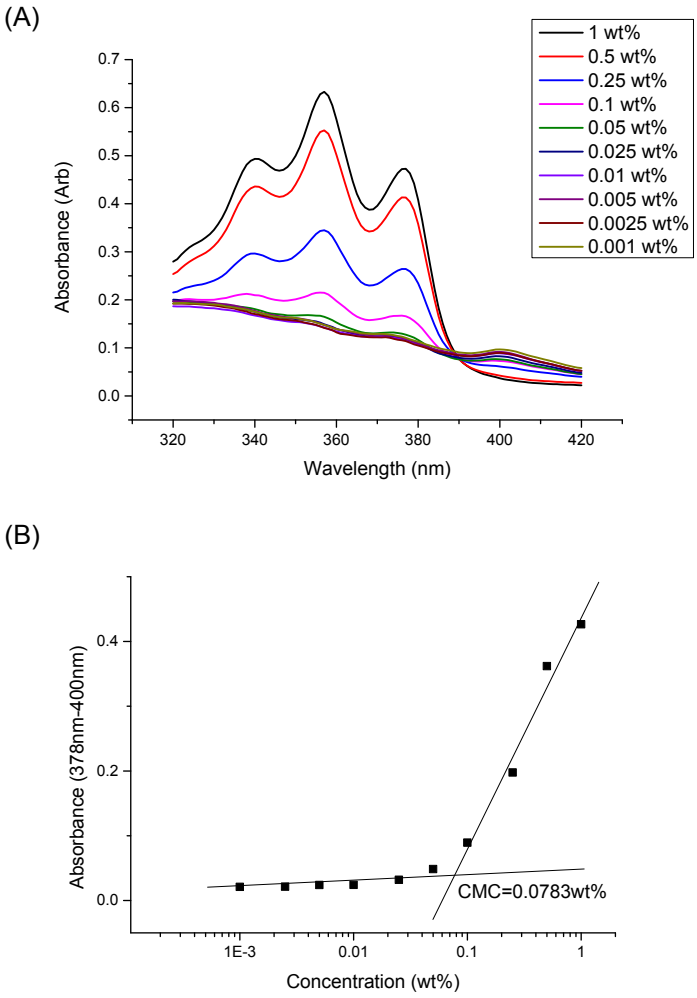

Figure S23. (A) UV-Vis absorbance spectra of DPH dye at different concentrations of polymer 1P35-4h at 35°C; (B) Difference in DPH absorbance at 378 and 400 nm as a function of concentration of 1P35-4h at 35°C. The CMC was determined by the intersection of the extrapolated linear best fit lines at low and high concentrations of polymer.

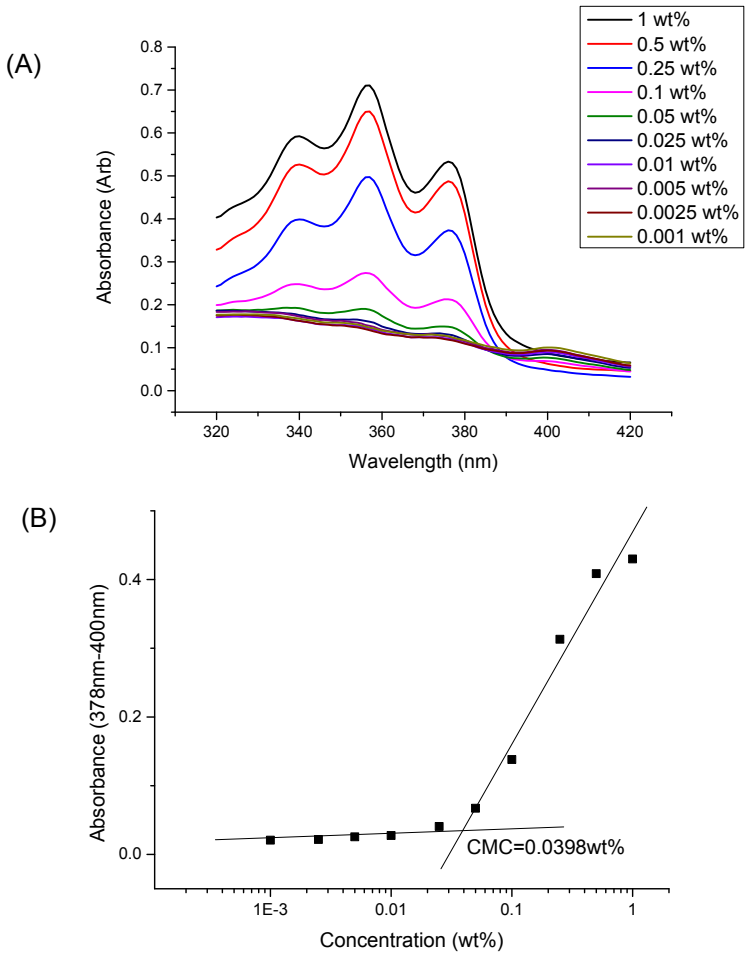

Figure S24. (A) UV-Vis absorbance spectra of DPH dye at different concentrations of polymer 1P35-4h at 45°C; (B) Difference in DPH absorbance at 378 and 400 nm as a function of concentration of 1P35-4h at 45°C. The CMC was determined by the intersection of the extrapolated linear best fit lines at low and high concentrations of polymer.

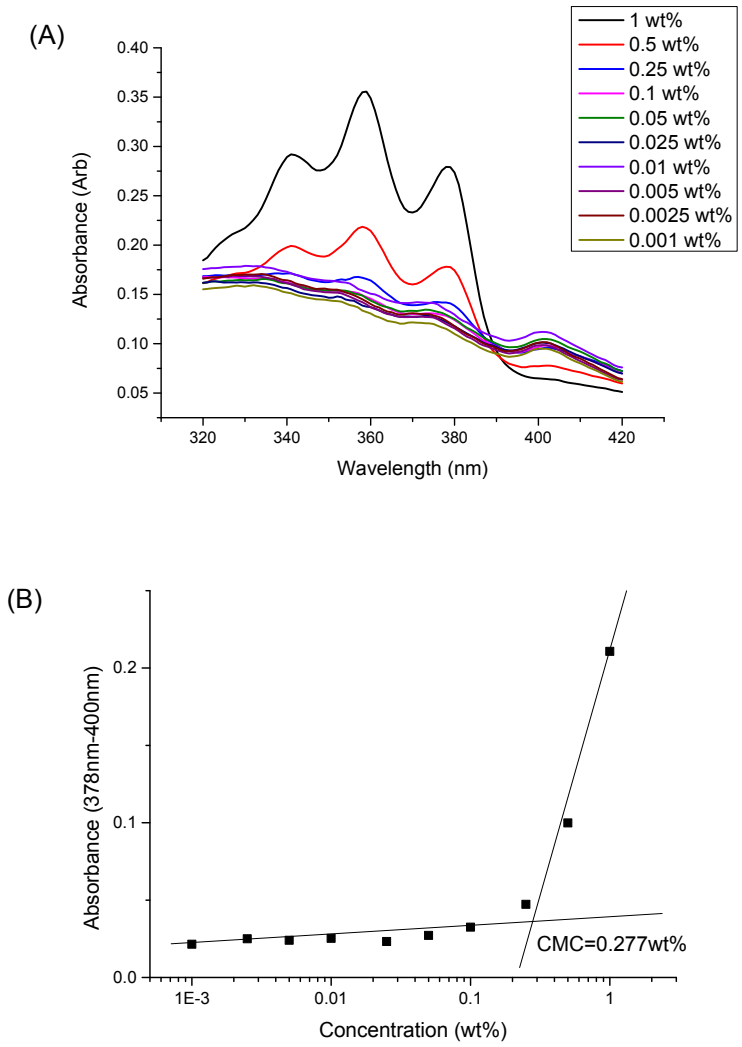

Figure S25. (A) UV-Vis absorbance spectra of DPH dye at different concentrations of polymer 1P40-1h at 15°C; (B) Difference in DPH absorbance at 378 and 400 nm as a function of concentration of 1P40-1h at 15°C. The CMC was determined by the intersection of the extrapolated linear best fit lines at low and high concentrations of polymer.

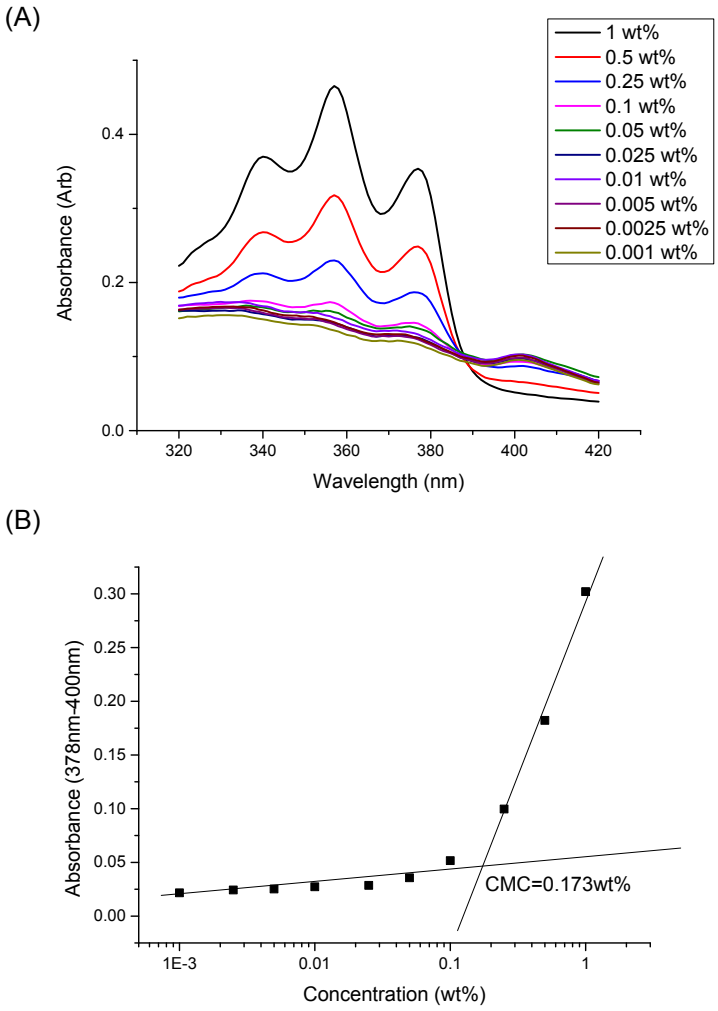

Figure S26. (A) UV-Vis absorbance spectra of DPH dye at different concentrations of polymer 1P40-1h at 25°C; (B) Difference in DPH absorbance at 378 and 400 nm as a function of concentration of 1P40-1h at 25°C. The CMC was determined by the intersection of the extrapolated linear best fit lines at low and high concentrations of polymer.

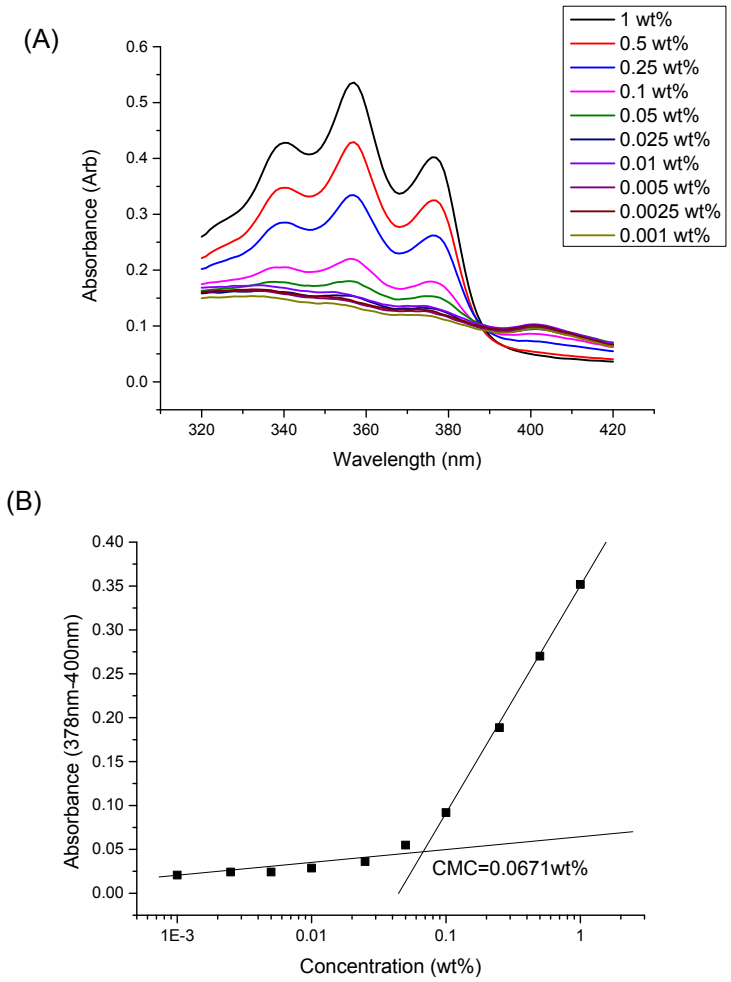

Figure S27. (A) UV-Vis absorbance spectra of DPH dye at different concentrations of polymer 1P40-1h at 35°C; (B) Difference in DPH absorbance at 378 and 400 nm as a function of concentration of 1P40-1h at 35°C. The CMC was determined by the intersection of the extrapolated linear best fit lines at low and high concentrations of polymer.

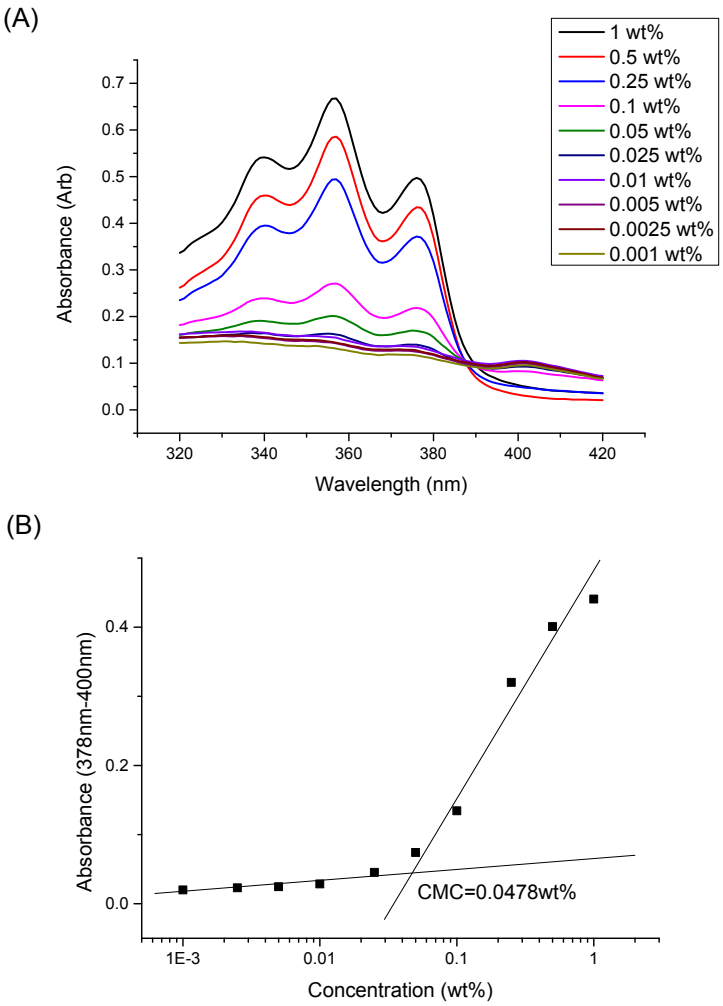

Figure S28. (A) UV-Vis absorbance spectra of DPH dye at different concentrations of polymer 1P40-1h at 45°C; (B) Difference in DPH absorbance at 378 and 400 nm as a function of concentration of 1P40-1h at 45°C. The CMC was determined by the intersection of the extrapolated linear best fit lines at low and high concentrations of polymer.

S3. Thermodynamics of Micellization for Thermogelling Polyurethanes

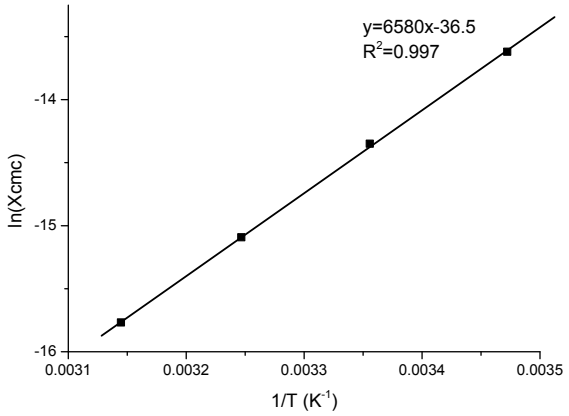

Figure S29. Arrhenius plot of $\ln(X_{CMC})$ as a function of T^{-1}/ K^{-1} for 1P30-2h.

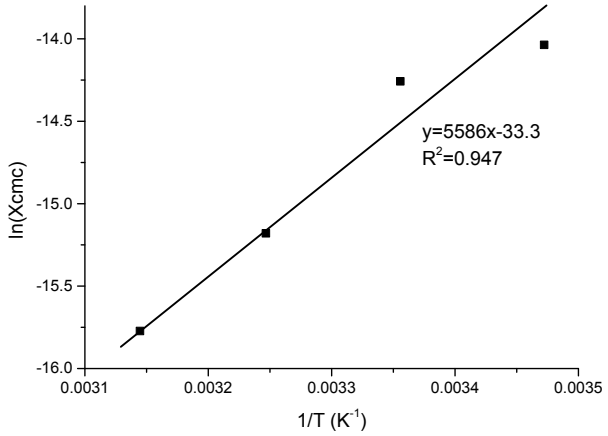

Figure S30. Arrhenius plot of $\ln(X_{CMC})$ as a function of T^{-1}/ K^{-1} for 1P30-3h.

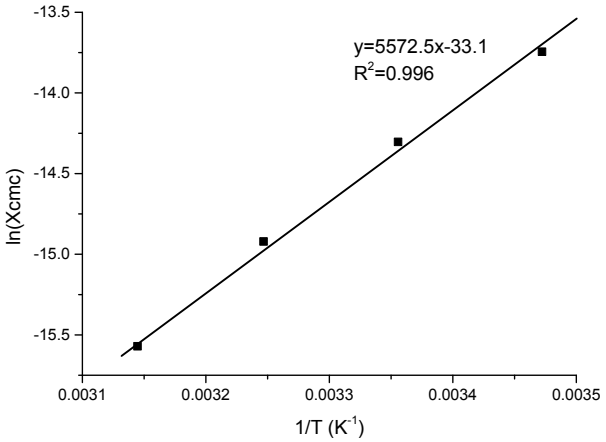

Figure S31. Arrhenius plot of $\ln(X_{CMC})$ as a function of T^{-1}/ K^{-1} for 1P35-2h.

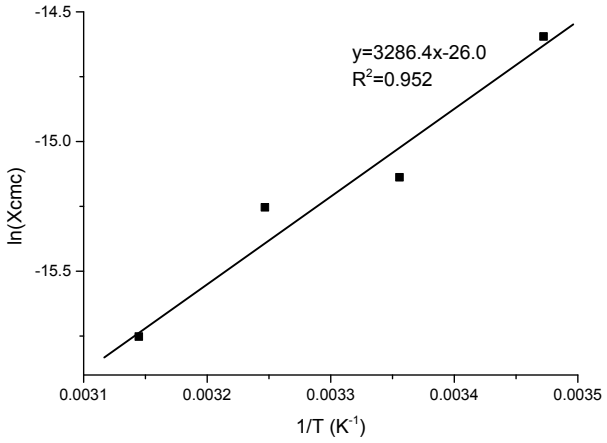

Figure S32. Arrhenius plot of $\ln(X_{CMC})$ as a function of T^{-1}/ K^{-1} for 1P35-3h.

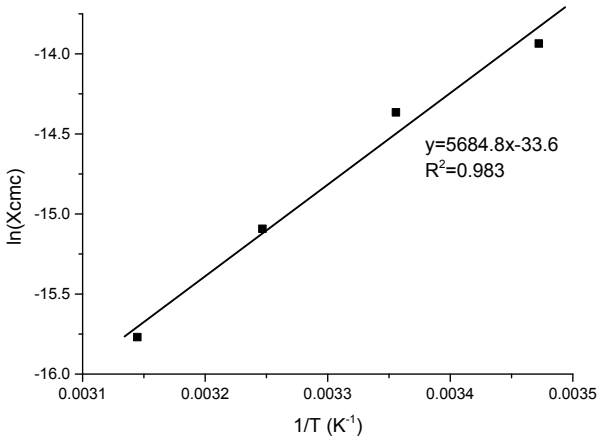

Figure S33. Arrhenius plot of $\ln(X_{CMC})$ as a function of T^{-1}/ K^{-1} for 1P35-4h.

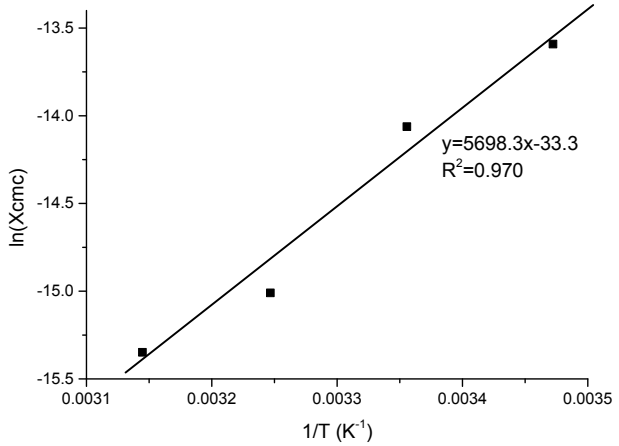

Figure S34. Arrhenius plot of $\ln(X_{CMC})$ as a function of T^{-1}/ K^{-1} for 1P40-1h.

S4. Temperature-sweep Rheology of Thermogelling Polyurethane Solutions

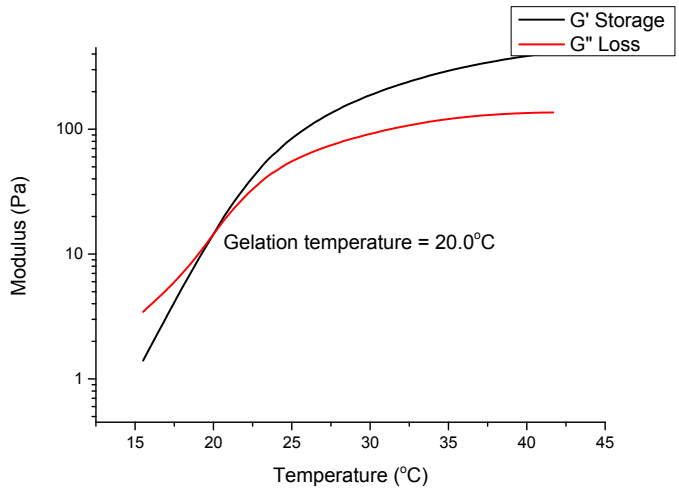

Figure S35. Changes in G' and G'' as a function of temperature for a 7 wt/v% solution of 1P30-2h in deionised water. Gelation occurs at the temperature when G' first exceeds G''.

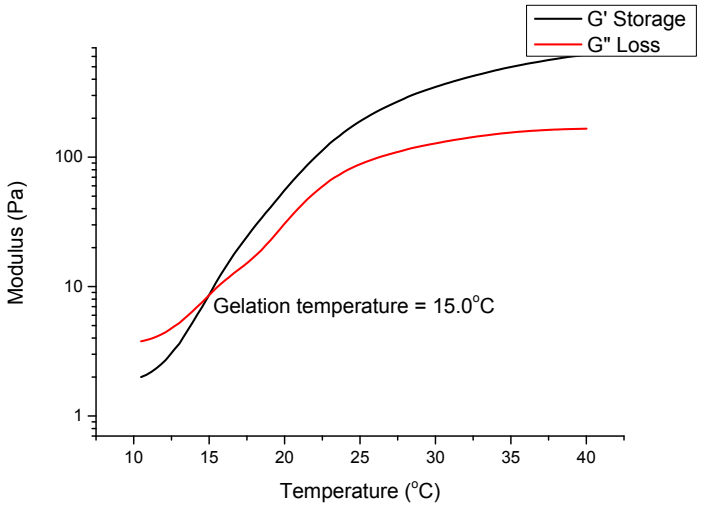

Figure S36. Changes in G' and G'' as a function of temperature for a 7 wt/v% solution of 1P30-3h in deionised water. Gelation occurs at the temperature when G' first exceeds G''.

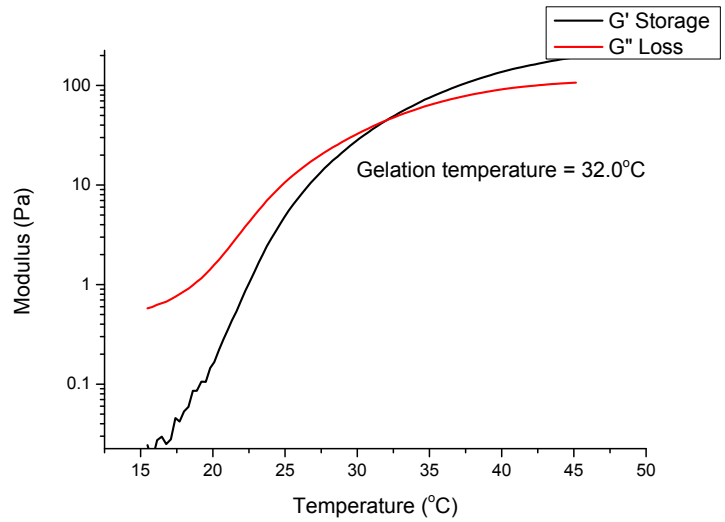

Figure S37. Changes in G' and G'' as a function of temperature for a 7 wt/v% solution of 1P35-1h in deionised water. Gelation occurs at the temperature when G' first exceeds G''

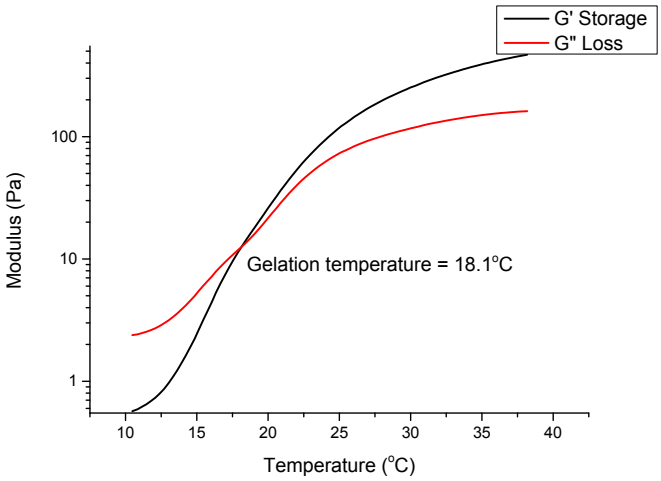

Figure S38. Changes in G' and G'' as a function of temperature for a 7 wt/v% solution of 1P35-2h in deionised water. Gelation occurs at the temperature when G' first exceeds G''

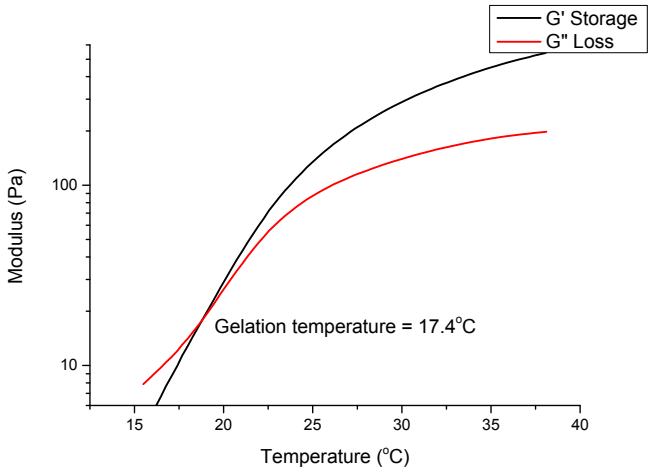

Figure S39. Changes in G' and G'' as a function of temperature for a 7 wt/v% solution of 1P35-3h in deionised water. Gelation occurs at the temperature when G' first exceeds G'',

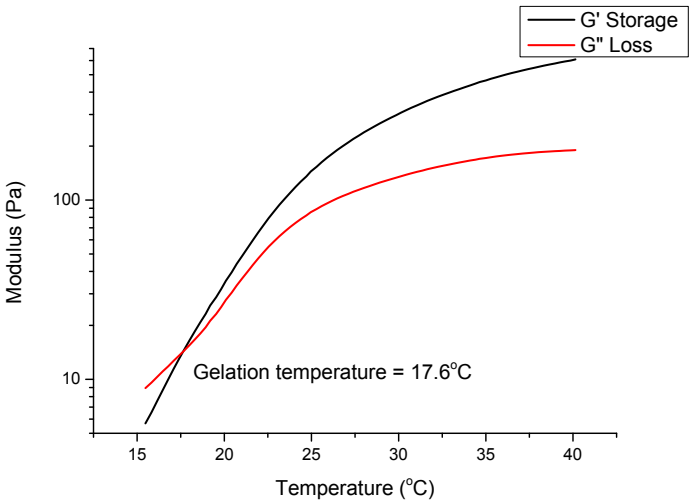

Figure S40. Changes in G' and G'' as a function of temperature for a 7 wt/v% solution of 1P35-4h in deionised water. Gelation occurs at the temperature when G' first exceeds G'',

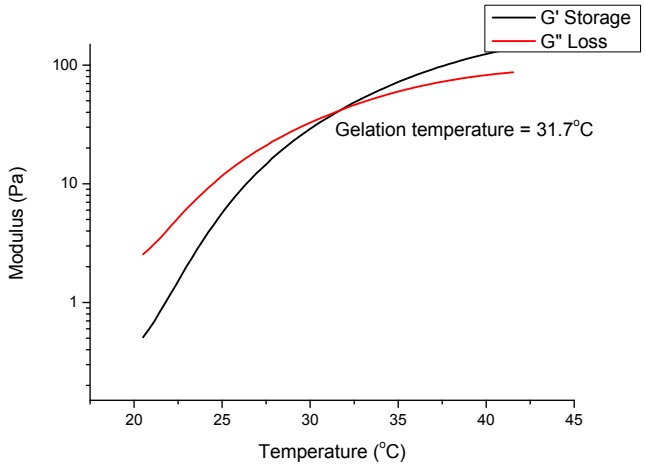

Figure S41. Changes in G' and G'' as a function of temperature for a 7 wt/v% solution of 1P40-1h in deionised water. Gelation occurs at the temperature when G' first exceeds G'',

S5. Degree of Branching

Derivation of H_c

The polymer structure may be written as (HMDI + PEG + PPG + PCL)$_n$, where n = no. of repeating units making up the main polymer chain as well as its branches.

The terms H, E, P and C are the average mole ratios of HMDI, PEG, PPG and PCL respectively per repeating unit.

Thus, n = $\frac{M_n}{H(168.19) + E(2050) + P(2000) + C(2000)}$, where the numbers in parentheses represent the molecular weights of each (macromonomer) component.

Moles of excess HMDI per repeating unit x_H = H – E – P – C

Total quantity of NCO-terminated branches per polymer = total quantity of excess HMDI present (as explained in the main text) = $nx_H = \frac{M_n}{H(168.19) + E(2050) + P(2000) + C(2000)} \times (H - E - P - C)$

Thus, quantity of NCO-terminated branches (H_c) = $\frac{1}{M_n} \times \frac{M_n}{H(168.19) + E(2050) + P(2000) + C(2000)} \times (H - E - P - C)$

$= \frac{H - E - P - C}{H(168.19) + E(2050) + P(2000) + C(2000)}$

Procedure for titration experiments to determine OH_c

An accurately-weighed sample of the poly(PEG/PPG/PCL urethane) polymer (typically ~0.4g) was dissolved in anhydrous DMSO (8.0 mL) at 80 °C. Separately, solutions of 4-dimethylaminopyridine (DMAP) and acetic anhydride (Ac_2O) were prepared in anhydrous DMSO at concentrations of 50 mg/mL and 50 µL/mL respectively. To the vigorously-stirred polymer solution was added 1 mL of DMAP and Ac_2O successively, and the reaction was left to stir at 80 °C for a further 1 hour. Thereafter, the

reaction was transferred quantitatively (washed with 3 x 5 mL DI water) to a conical flask containing chilled DI water and chilled further to ensure a homogeneous solution was obtained. Thereafter, the contents were heated to 80 °C for a further 20 minutes to ensure complete hydrolysis of Ac_2O. Upon cooling of the solution to ambient temperature, 1 mL of 1wt% phenolphthalein indication was added and mixed thoroughly. The solution was titrated with 30 mM NaOH (aq) until a persistent pink coloration was observed. The volume of NaOH (aq) used was V_p.

For the blank control, the procedure was repeated as above except that the polymer was substituted with 1 mL of DI water for complete hydrolysis of Ac_2O. The volume of 30 mM NaOH required for titration of the resulting eventual acetic acid solution is V_b.

Derivation of OH_c

Less acetic acid (AcOH) is produced in the presence of the polymer than in the blank control reaction. The difference is equivalent to the quantity of alcohol (ROH) groups present = $(V_b - V_p) \times C$, where C = concentration of NaOH (aq).

The no. of ROH groups per unit mass of polymer = $\frac{1}{M} \times (V_b - V_p) \times C$, where M = accurate mass of polymer sample used for titration.

As this procedure does not differentiate between OH groups on either the main polymer chain or on the branches, the OH of the main polymer chain can be taken into account by subtracting $\frac{1}{M_n}$ from this value, to give $OH_c(molg^{-1}) = \left(\frac{1}{M} \times (V_b - V_p) \times C\right) - \frac{1}{M_n}$.

In all cases, however, $\frac{1}{M_n}$ is very small compared to the term in parentheses.

Table S2. Determination of quantity of branches per unit mass of each polymer investigated

Polymer	NCO-terminated branches						OH-terminated branches			Total branches/ (10^{-4} mol g^{-1}) [b]
	H	E	P	C	X_H[a]	H_c/ (10^{-6} mol g^{-1})	V_b/ mL	V_p/ mL	OH_c / (10^{-4} mol g^{-1})	
1P30 1h	5.45	4.38	1	0.0516	0.0175	1.46	21.1	15.9	4.59	4.6
1P30 2h	5.13	4.06	1	0.0548	0.00836	0.740	21.5	16.9	3.69	3.7
1P30 3h	5.52	4.18	1	0.0490	0.292	25.2	21.1	16.3	4.45	4.7
1P35 1h	5.64	4.48	1	0.0522	0.106	8.65	18.8	16.6	1.61	1.7
1P35 2h	5.62	4.21	1	0.0458	0.371	31.9	20.9	18.1	2.28	2.6
1P35 3h	5.67	4.19	1	0.0399	0.441	38.0	18.8	15.8	2.42	2.8
1P35 4h	5.66	4.20	1	0.0414	0.414	35.5	21.5	16.4	3.55	3.9
1P40 1h	5.59	4.33	1	0.0559	0.209	17.5	21.5	16.8	3.63	3.8

[a] $X_H = H - E - P - C$; [b] Total branches = $H_c + OH_c$